Strength, Fracture and Complexity 13 (2020) 105–114
DOI 10.3233/SFC-200259
IOS Press

Fractal scaling and specimen-size effects on creep resistance

Alberto Carpinteri, Gianni Niccolini and Alessio Rubino*
Department of Structural, Geotechnical and Building Engineering, Politecnico di Torino, Corso Duca degli Abruzzi 24, Torino, Italy

Received 27 July 2020
Accepted 31 August 2020

Abstract. Scaling effects governing the creep behaviour of unnotched and uncracked metallic specimens are investigated by applying similarity considerations and fractal modelling to experimental results provided in the literature. The focus is on stress rupture tests conducted at elevated temperatures on Cr-Mo-V steel cylindrical bars of different sizes. The observed specimen-size effects on the σ versus t_R creep resistance diagrams are interpreted in terms of incomplete self-similarity and fractal weakening (lacunarity) of the specimen reacting cross-section. That leads to a scale-invariant (fractal) formulation of the creep rupture law in terms of renormalized stress.

Keywords: Creep rupture, scaling effects, incomplete self-similarity, fractal geometry, renormalization group theory

1. Introduction

An important issue in the life assessment of structural components operating at elevated temperatures is to characterize the creep deformation. Creeping materials tend to undergo time-dependent plastic deformations as a result of long-term exposure to high levels of stress that are still below the yield strength of the material. The major part of the creep life is consumed under steady-state conditions, which are characterized by a strain rate $\dot{\varepsilon}$ constant in time according to the Norton law, i.e. the secondary creep law [23,38]:

$$\dot{\varepsilon} = A\sigma^n, \tag{1}$$

where σ is the applied stress, while A and n are temperature-dependent material parameters. The latter, n, is the susceptibility to creep deformation or creep sensitivity, ranging typically from 3 to 15 for metals and being close to unity for polymers [31].

A fundamental relationship for creep-resistant materials design is found by means of stress rupture tests, conducted in a similar way as typical uniaxial creep tests, although aimed at determining the stress which, at a given temperature, will cause material failure in a given time. Thus, an inverse power-law

*Corresponding author: Alessio Rubino. E-mail: alessio.rubino@polito.it.

Table 1
Values of the average exponents 1 p

T (°C)	1 p
482	0.07 ± 0.01
538	0.099 ± 0.003
593	0.17 ± 0.03

relationship between the time-to-rupture t_R and the applied stress σ can approximate the stress sensitivity of the time-to-rupture t_R [38]:

$$t_R = B\sigma^{-p}, \tag{2}$$

where B and p are temperature-dependent material parameters.

This relationship shows a strong analogy with the Basquin law for fatigue [4,39], since in both cases an increase in the applied stress levels results in a reduction of the component life.

Here, a rather remarkable analogy between such delayed failure mechanisms, creep and fatigue [12–17,19,21,22,25,28–30,35], is established, whereby analogous scaling effects are observed and similarly shaped curves are emerging.

2. Specimen-size effects on creep rupture time

In the assessment of high-temperature material behaviour for design considerations, size effects on stress rupture properties have been demonstrated. A specimen-size effect was experimentally verified by Goldhoff [24] on Cr-Mo-V steel specimens subjected to stress rupture tests. Cylindrical bars were tested in uniaxial tension at temperatures ranging from 482 °C to 593 °C. Test section diameters of the specimens were 0.160, 0.253, 0.505, and 1.128 in., spanning one order of magnitude. Though both smooth and notched bars were tested, the current paper focuses on pure specimen-size effects. Thus, only the results on smooth bars are reported and discussed, so as to exclude the constraint effects affecting the creep crack propagation in notched specimens [32–34,36,37,41–45]. Such effects are due to loading configuration [36,41,44], crack depth (in-plane constraint effects) [32,37,42], and specimen thickness (out-of-plane constraint effects) [33,34].

The overall results of this study are shown in Fig. 1, representing stress rupture diagrams for different specimen sizes and temperatures. Each point depicts the result of a single test conducted on a bar of diameter b held at a given temperature T. The logarithmic representation of $\sigma = \sigma(t_R)$ yields a set of almost parallel lines for each temperature condition, where the slope 1 p is equal to 1 15 at 482 °C, 1 10 at 538 °C and 1 6 at 593 °C (also see Table 1). Looking at Fig. 1, the stresses necessary to produce failure in a given rupture time at 482 °C are on average larger by a factor $10^{0.15}$ 1.4 than those at 538 °C and by $10^{0.3}$ 2 than those at 593 °C.

Besides the expected dependence of creep strength on temperature —creep becomes severe when the absolute operating temperature T exceeds 40% of the absolute melting temperature T_M of the material— a size effect appeared as well. The downward shift of the stress rupture curves for increasing specimen size b is emphasized in Fig. 2 revealing a systematic, although small, decrease in strength with size.

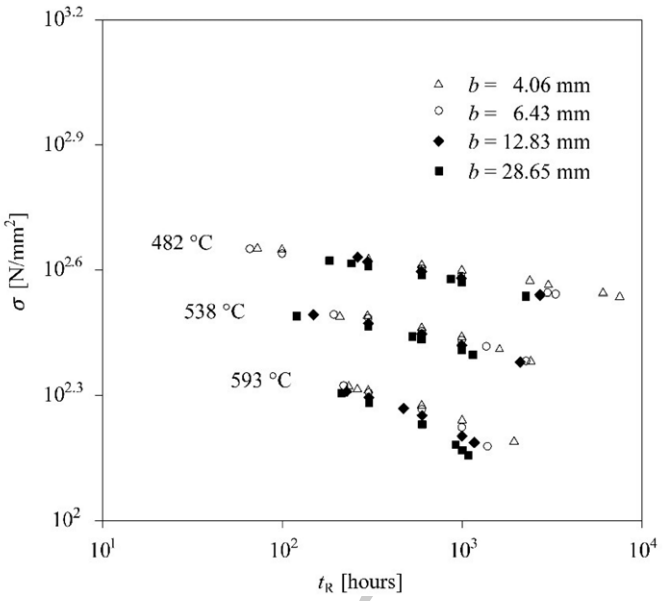

Fig. 1. Experimental stress rupture diagrams at different temperature conditions for smooth specimens of various sizes (adapted from [24]).

Actually, one case —for a steel with slightly differing chemical composition— provided a controversial finding, whereby the increasing size caused an increase in creep strength. This evidence is in contradiction with well-known size effects on tensile strength, and makes experimental investigations much-needed in the future.

3. Generalized creep rupture law

The above results give the evidence of poor information provided by Eq. (2) on the multiple factors affecting the creep rupture of a material. Furthermore, there is considerable evidence for the presence of a threshold stress (or creep limit), σ_{th}, in the high temperature creep regime of metals [6–8,27], below which no measurable strain rate can be achieved. Thus, deviations from the power-law behaviour of Eq. (2) are expected both at high values of σ close to the ultimate tensile strength σ_u, and at low values of σ close to the creep limit condition, σ_{th}, yielding the typical Wöhler-type stress rupture diagram of Fig. 3.

Therefore, assuming that t_R depends on multiple parameters, the following functional dependence can be stated:

$$t_R = \Psi(\sigma, T; \sigma_u, \sigma_{th}, K_C, X, T_M; b), \tag{3}$$

where b is the characteristic specimen size and X is the thermal diffusivity (m^2 s ^{1}), which controls the migration of vacancies responsible for creep.

Taking K_C, σ_u, X, and T_M as independent variables, an application of the Buckingham π theorem [5] gives:

$$t_R = \frac{a_0^2}{X}\Psi_1\left(\frac{\sigma}{\sigma_u}, \frac{\sigma_{th}}{\sigma_u}, \frac{T}{T_M}, \frac{b}{a_0}\right), \tag{4}$$

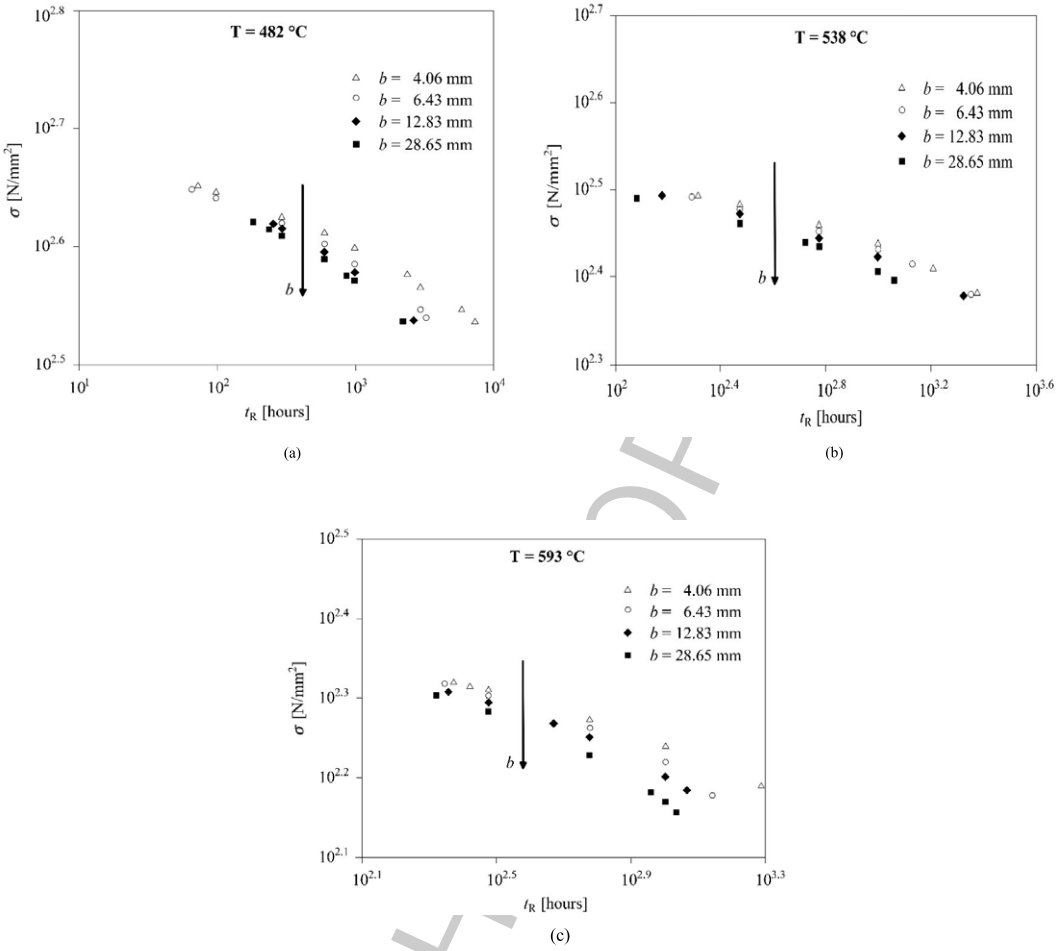

Fig. 2. (a–c) Dependence of rupture time on stress as a function of specimen size (adapted from [24]).

where the fracture toughness K_C and the tensile strength σ_u of the material are expressed through the fracture sensitivity $a_0 = (K_C \ \sigma_u)^2 \ \pi$.

Based on self-similarity considerations [1–3], the power-law range of the stress-rupture diagram is regarded as an intermediate-asymptotic stage, wherein the process is sufficiently far from both creep limit and ultimate tensile conditions. The so-called incomplete self-similarity prevails at this stage corresponding to a power-law dependence of rupture time t_R on certain dimensionless parameters.

The experimentally proved dependencies on the applied stress σ and the specimen size b lead to assume incomplete self-similarity in the corresponding dimensionless parameters $\sigma \ \sigma_u$ and $b \ a_0$ for the mid-range of rupture times, i.e. when $\sigma_{th} \quad \sigma \quad \sigma_u$. Accordingly, Eq. (4) has the following power-law asymptotic representation:

$$t_R = \frac{a_0^2}{X}\Psi_2\left(\frac{\sigma_{th}}{\sigma_u}, \frac{T}{T_M}\right)\left(\frac{b}{a_0}\right)^{\delta_2}\left(\frac{\sigma}{\sigma_u}\right)^{\delta_1} \equiv B\sigma^{\delta_1}, \tag{5}$$

where the effects of temperature are accounted for in the function Ψ_2.

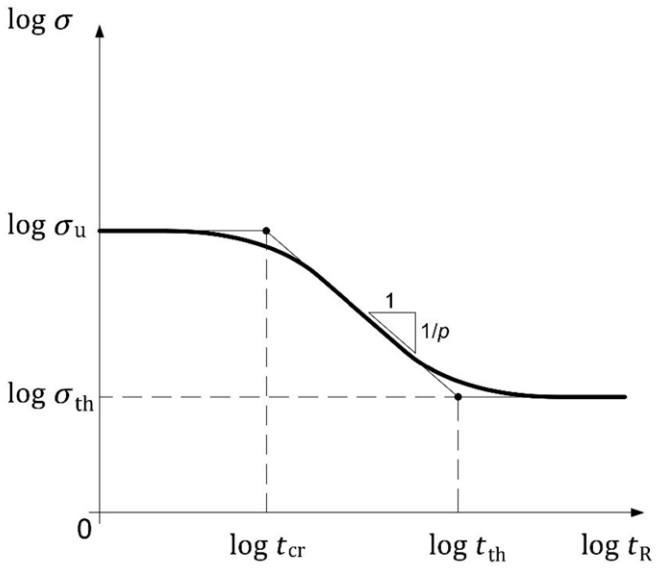

Fig. 3. Schematization of a stress rupture diagram: power-law stage corresponds to the intermediate asymptotic behaviour.

By comparing Eqs (2) and (5), it immediately results that $\delta_1 = p$. Furthermore, from Eq. (5) it is apparent that B is not simply a function of the material properties and the temperature, but also of the specimen size b, where the exponent δ_2 governing the size effect cannot be obtained by dimensional analysis, but rather has to be calibrated from the experimental data.

4. Fractal creep rupture law

As reported in a celebrated work by Mandelbrot et al. [26], the experiments have revealed the fractal character of metals' structure, where observations at various magnification scales show a variety of self-similar structures, falling between the micro-scale (characterized by grains and inclusions) and the macro-scale (defined by specimen and notch sizes). Such a fractal nature is also present in metallic substructures under creep conditions due to the self-similar pattern of moving dislocations responsible for the phenomenon [20,40]. Thus, it can be inferred that the observed shift of the σ versus t_R curves can be interpreted in terms of fractal weakening (lacunarity) of the material ligament, which is modeled as a fractal set of topological dimension $2 - d_\sigma$, with $0 < d_\sigma < 1$ [9–11,18]. An extension of the scaling law for the nominal tensile strength, $\sigma_u = \sigma_u^* b^{-d_\sigma}$, to generic stress values gives $\sigma = \sigma\ b^{-d_\sigma}$. Inserting this relation into Eq. (2) leads to the following scale-invariant, or fractal, law:

$$t_R = B^* \sigma^{*-p}, \tag{6}$$

establishing that a given time-to-rupture t_R results from a size-independent renormalized stress σ with anomalous physical dimensions $[F][L]^{(2-d_\sigma)}$, where B is solely temperature and material dependent:

$$B^* \equiv B b^{d_\sigma p}. \tag{7}$$

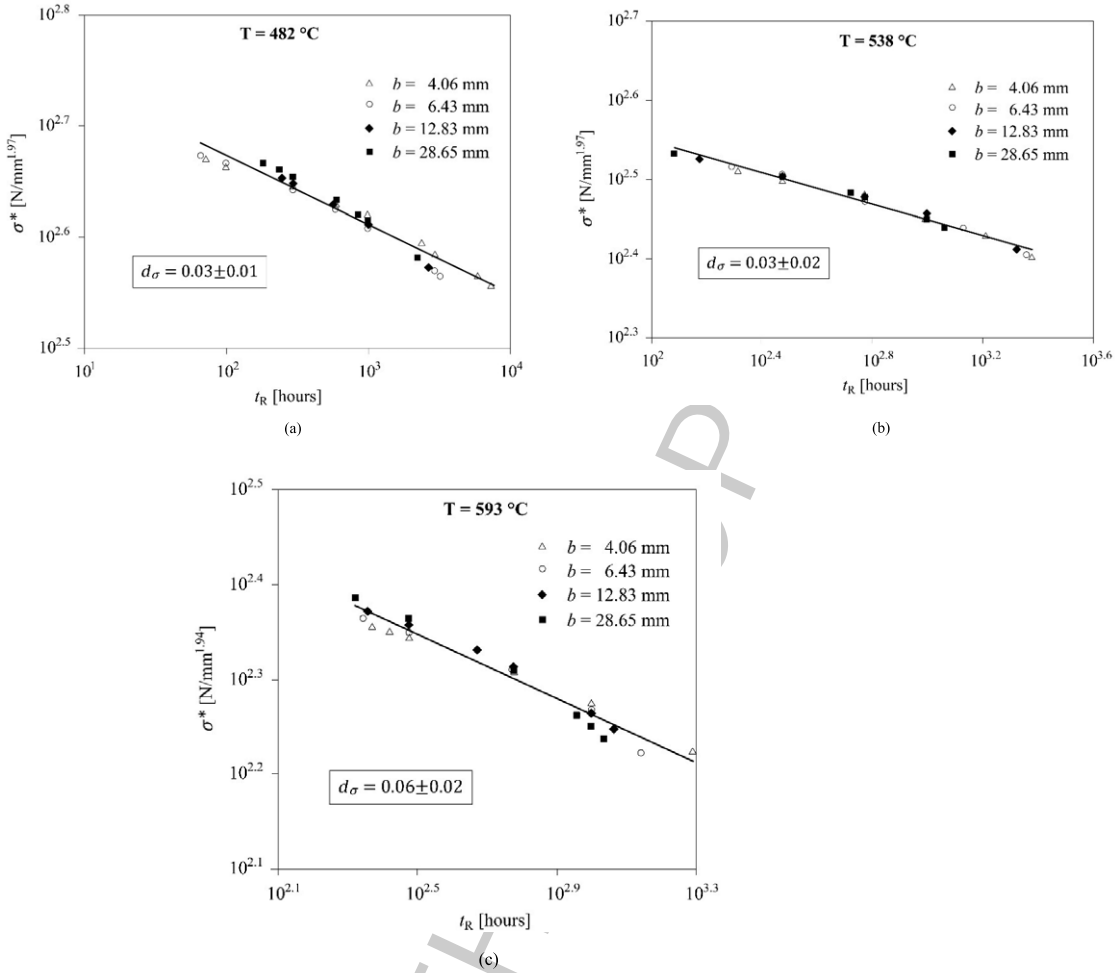

Fig. 4. (a–c) Renormalized stress rupture curves. The fitting function is the scaling function $\sigma^* = B^{*1/p} t_R^{-1/p}$, which is obtained from Eq. (6).

Using Eq. (7), Eq. (2) can be written as:

$$t_R = B^* b^{-d_\sigma p} \sigma^{-p}, \tag{8}$$

or in logarithmic form:

$$\log \sigma = \frac{1}{p} \log B^* - d_\sigma \log b - \frac{1}{p} \log t_R. \tag{9}$$

This expression shows that the stress σ expected to cause rupture in a given time t_R decreases as the specimen size b increases, at a rate governed by d_σ.

Further considerations can be made by comparing the results of fractal and self-similarity approaches to the stress rupture law. From Eqs (5) and (8), the following relationship is easily obtained:

$$B \equiv \frac{a_0^2}{X} \Psi_2 \left(\frac{\sigma_{th}}{\sigma_u}, \frac{T}{T_M} \right) \left(\frac{b}{a_0} \right)^{\delta_2} \sigma_u^{-\delta_1} = B^* b^{-d_\sigma p}, \tag{10}$$

Table 2
Fitting parameters of the scaling function $\sigma^* = B^{*1/p} t_R^{-1/p}$ of Fig. 4

T (°C)	log$B$ ( )	1 p
482	45.1	0.062
538	27.8	0.098
593	16.3	0.17

B is expressed in N^p mm $^{(2\ d_\sigma)p}$ h.

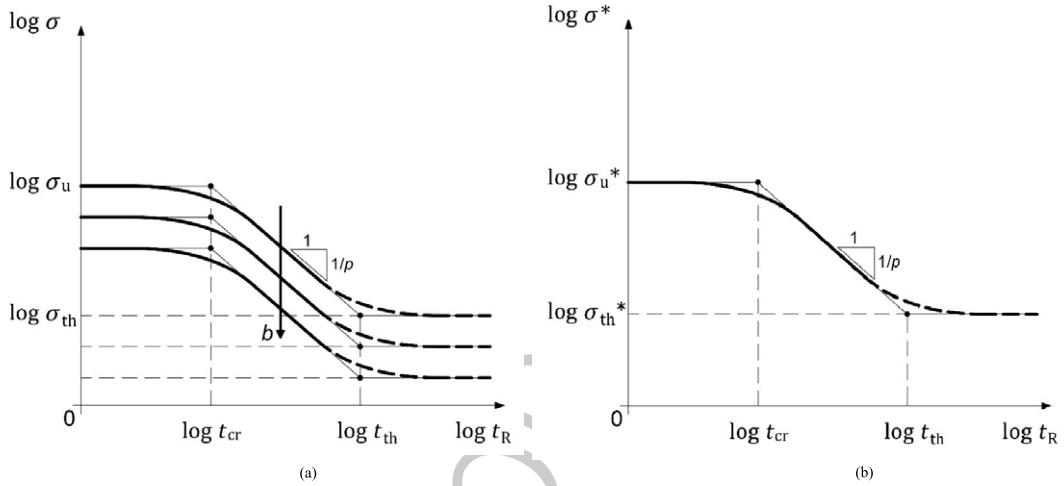

Fig. 5. Predicted shift of the nominal stress rupture curves (a); collapse of the renormalized curves in the fractal diagram (b). The dashed branches depict the asymptotic behaviour to be investigated.

which yields:

$$\delta_2 = -d_\sigma p. \tag{11}$$

Then, the experimental stress rupture curves are renormalized by subjecting stress data to the following transformation, $\sigma \rightarrow \sigma = \sigma b^{d_\sigma}$. The renormalized curves collapse onto a single line for each temperature condition, as shown in Fig. 4, illustrating the fulfilment of the specimen-size independent scaling law of Eq. (6). The fitting line for the diagrams of Fig. 4 is represented by the scaling function $\sigma^* = B^{*1/p} t_R^{-1/p}$.

The optimized exponent d_σ yielding the best data collapse is equal to 0.03 ± 0.01 at 482 °C, 0.03 ± 0.02 at 538 °C, and 0.06 ± 0.02 at 593 °C. It can be observed that the statistical discrepancy is not significant, i.e. the single values of d_σ are compatible among themselves, as the stated error bars overlap. The fitting parameters 1 p and B are reported in Table 2.

5. Discussion and conclusions

In this work, specimen-size effects on the creep strength are discussed, considering stress rupture diagrams obtained from uniaxial creep tests conducted on steel bars of different sizes [24]. Although

the experimental campaign originally regarded both smooth and notched cylindrical bars, in this paper the analysis is restricted to smooth specimens, in order to exclude the constraint effects related to the propagation of a pre-existing crack under creep conditions. Under these circumstances, dimensional analysis and self-similarity considerations provide a generalized representation of the creep rupture law, where dependencies on multiple parameters and deviations from the mid-range power-law regime can be taken into account. In this framework, the observed size effect on the creep strength is signature of incomplete self-similarity in the specimen size.

The geometrical meaning of the aforementioned size effects and incomplete self-similarity is rooted in the fractal geometry of specimen cross-section. The severity of the size effect is related to the microstructural disorder through the dimensional decrement d_σ of the material ligament.

Similarly to static and fatigue failures, the renormalized creep strength is introduced as an intrinsic property of the material, leading to the definition of a fractal (scale-invariant) creep rupture law. As ultimate tensile strength and creep limit conditions are approached, deviations from the mid-range power-law regime are expected both in nominal and fractal diagrams. In particular, assuming for the creep limit σ_{th} the same scaling effect as for σ_u and σ, i.e. $\sigma_{th} = \sigma^*_{th} b^{-d_\sigma}$, yields the downward shift of the Wöhler-type curves and the collapse of the renormalized curves, as represented respectively in Figs 5(a) and (b). The emerging leitmotiv would be the strong analogy between the sub-critical failure mechanisms of creep and fatigue. Indeed, similarly shaped curves may depict analogous scaling laws, which are obtained from each other by the change of variable $N \leftrightarrow t$ (number of cycles $\leftrightarrow$ time).

Extensive experimental work should be conducted to confirm the present approach. With specific reference to the creep limit σ_{th}, the greatest difficulty really seems to consist in the extremely long-term tests in order to ascertain the existence of the conjectured asymptotic behaviour (represented in Fig. 5).

Conflict of interest

None to report.

References

[1] G.I. Barenblatt, *Scaling, Self-similarity and Intermediate Asymptotics*, Cambridge University Press, Cambridge, 1996.
[2] G.I. Barenblatt, Scaling phenomena in fatigue and fracture, *International Journal of Fracture* **138** (2006), 19–35.
[3] G.I. Barenblatt and L.R. Botvina, Incomplete self-similarity of fatigue in the linear range of fatigue crack growth, *Fatigue and Fracture of Engineering Materials and Structures* **3** (1980), 193–202.
[4] O.H. Basquin, The exponential law of endurance tests, *Proceedings ASTM* **10** (1910), 625–630.
[5] E. Buckingham, Model experiments and the forms of empirical equations, *ASME Transactions* **37** (1915), 263–296.
[6] J. Cadek and V. Sustek, Comment on steady state creep behaviour of silicon carbide reinforced aluminium composites, *Scripta Metall. Mater.* **30** (1994), 277–282.
[7] J. Cadek, H. Oikawa and V. Sustek, Threshold creep behaviour of discontinuous aluminium and aluminium alloy matrix composites: An overview, *Material Science and Engineering A* **190**(1–2) (1995), 9–23.
[8] J. Cadek, V. Sustek and M. Pahutova, Is creep in discontinuous metal matrix composites lattice diffusion controlled? *Material Science and Engineering A* **174** (1994), 141–147.
[9] A. Carpinteri, Size effects on strength, toughness and ductility, *Journal of Engineering Mechanics* **115** (1989), 1375–1392.
[10] A. Carpinteri, Fractal nature of material microstructure and size effects on apparent mechanical properties, *Mechanics of Materials* **18** (1994), 89–101, Internal Report, Laboratory of Fracture Mechanics, Politecnico di Torino, N. 1/92, 1992.
[11] A. Carpinteri, Scaling laws and renormalization groups for strength and toughness of disordered materials, *International Journal of Solids and Structures* **31** (1994), 291–302.

[12] A. Carpinteri and F. Montagnoli, Scaling and fractality in fatigue crack growth: Implications to Paris' law and Wöhler's curve, *Procedia Structural Integrity* **14** (2019), 957–963.
[13] A. Carpinteri, F. Montagnoli and S. Invernizzi, Scaling and fractality in fatigue resistance: Specimen-size effects on Wöhler's curve and fatigue limit, *Fatigue & Fracture of Engineering Materials & Structures* **43**(8) (2020), 1869–1879.
[14] A. Carpinteri and M. Paggi, A unified interpretation of the power laws in fatigue and the analytical correlations between cyclic properties of engineering materials, *International Journal of Fatigue* **31** (2009), 1524–1531.
[15] A. Carpinteri and M. Paggi, A unified fractal approach for the interpretation of the anomalous scaling laws in fatigue and comparison with existing models, *International Journal of Fracture* **161** (2010), 41–52.
[16] A. Carpinteri and M. Paggi, Dimensional analysis and fractal modeling of fatigue crack growth, *Journal of the ASTM International* **8** (2011), 1–13.
[17] A. Carpinteri and M. Paggi, The effect of crack size and specimen size on the relation between the Paris and Wöhler curves, *Meccanica* **49** (2014), 765–773.
[18] A. Carpinteri and A. Spagnoli, Size effect in S-N curves: A fractal approach to finite-life fatigue strength, *International Journal of Fatigue* **31** (2009), 927–933.
[19] W. Cui, A state-of-the-art review on fatigue life prediction methods for metal structures, *Journal of Marine Science and Technology* **7** (2002), 43–56.
[20] R. Fernández, G. Bruno and G. González-Doncel, Fractal nature of aluminum alloys substructures under creep and its implications, *Journal of Applied Physics* **123** (2018), 145108-1–145108-8.
[21] Y. Furuya, Size effects in gigacycle fatigue of high-strength steel under ultrasonic fatigue testing, *Procedia Engineering* **2** (2010), 485–490.
[22] Y. Furuya, Notable size effects on very high cycle fatigue properties of high-strength steel, *Materials Science and Engineering A* **528** (2011), 5234–5240.
[23] F. Garofalo, *Fundamentals of Creep and Creep-Rupture in Metals*, Macmillan Series in Materials Science, 1965.
[24] R. Goldhoff, Stress concentration and size effects in a Cr-Mo-V steel at elevated temperatures, *Proceedings of the Institution of Mechanical Engineers* **178** (1963), 19–32.
[25] K. Hatanaka, S. Shimizu and A. Nagae, Size effect on rotating bending fatigue in steels, *Bulletin of the JSME* **26** (1983), 1288–1295.
[26] B.B. Mandelbrot, D.E. Passoja and A.J. Paullay, Fractal character of fracture surfaces of metals, *Nature* **308** (1984), 721–722.
[27] V.C. Nardone and J.R. Strife, Analyisis of the strength and fracture behaviour of unidirectional and angle-ply graphite-aluminium composites, *Journal of Material Science* **22** (1987), 592–600.
[28] O. Plekhov, M. Paggi, O. Naimark and A. Carpinteri, A dimensional analysis interpretation to grain size and loading frequency dependencies of the Paris and Wöhler curves, *International Journal of Fatigue* **33** (2011), 477–483.
[29] R.O. Ritchie, Incomplete self-similarity and fatigue-crack growth, *International Journal of Fracture* **132** (2005), 197–203.
[30] Y. Shirai, A.T. Yokobori, R. Sugiura, D. Fukuda, D. Matsuzaki, H. Ishikawa and K. Ito, The effect of load frequency on the temperature dependence of fracture life of notched specimens for 9–12 Cr steel under creep-fatigue conditions, in: *Proceedings of the ASME 2015 Pressure Vessels and Piping Conference, 19–23 July 2015, Boston, Massachusetts (USA)* 2015.
[31] D.J. Smith and G.A. Webster, Characterizations of creep crack growth in 1 per cent Cr Mo V steel, *Journal of Strain Analysis* **16**(2) (1981), 137–143.
[32] P.J. Sun, G.Z. Wang, F.Z. Xuan, S.T. Tu and Z.D. Wang, Quantitative characterization of creep constraint induced by crack depths in compact tension specimens, *Engineering Fracture Mechanics* **78**(4) (2011), 653–665.
[33] P.J. Sun, G.Z. Wang, F.Z. Xuan, S.T. Tu and Z.D. Wang, Three-dimensional numerical analysis of out-of-plane creep crack-tip constraint in compact tension specimens, *International Journal of Pressure Vessels and Piping* **96–97** (2012), 78–89.
[34] J.P. Tan, S.T. Tu, G.Z. Wang and F.Z. Xuan, Effect and mechanism of out-of-plane constraint on creep crack growth behavior of a Cr-Mo-V steel, *Engineering Fracture Mechanics* **99** (2013), 324–334.
[35] S. Usami, Applications of threshold cyclic-plastic-zone-size criterion to some fatigue limit problems, in: *Fatigue Threshold*, J. Bäcklund, A.F. Blom and C.J. Beevers (eds), vol. I, Engineering Material Advisory Services, Inc., Warley West Midlands, United Kingdom, 1982, pp. 205–238.
[36] G.Z. Wang, B.K. Li, F.Z. Xuan and S.T. Tu, Numerical investigation on the creep crack-tip constraint induced by loading configuration of specimens, *Engineering Fracture Mechanics* **79** (2012), 353–362.
[37] G.Z. Wang, X.L. Liu, F.Z. Xuan and S.T. Tu, Effect of constraint induced by crack depth on creep crack-tip stress field in CT specimens, *International Journal of Solids and Structures* **47**(1) (2010), 51–57.

[38] G.A. Webster and R.A. Ainsworth, *High Temperature Components Life Assessment*, Chapman and Hall, London, 1994.
[39] A. Wöhler, Versuche über die Festigkeit Eisenbahnwagenuchsen, *Z. Bauwesen* **10** (1860).
[40] M. Zaiser, K. Bay and P. Hähner, Fractal analysis of deformation-induced dislocation patterns, *Acta Mater.* **47** (1999), 2463–2476.
[41] J.W. Zhang, G.Z. Wang, F.Z. Xuan and S.T. Tu, Prediction of creep crack growth behavior in Cr-Mo-V steel specimens with different constraints for a wide range of C^*, *Engineering Fracture Mechanics* **132** (2014), 70–84.
[42] L. Zhao, H. Jing, L. Xu, Y. Han and J. Xiu, Evaluation of constraint effects on creep crack growth by experimental investigation and numerical simulation, *Engineering Fracture Mechanics* **96** (2012), 251–266.
[43] L. Zhao, H. Jing, J. Xiu, Y. Han and L. Xu, Experimental investigation of specimen size effect on creep crack growth behavior in P92 steel welded joint, *Materials and Design* **57** (2014), 736–743.
[44] L. Zhao, L. Xu, Y. Han and H. Jing, Quantifying the constraint effect induced by specimen geometry on creep crack growth behavior in P92 steel, *International Journal of Mechanical Sciences* **94–95** (2015), 63–74.
[45] L. Zhao, L. Xu, Y. Han and H. Jing, Two-parameter characterization of constraint effect induced by specimen size on creep crack growth, *Engineering Fracture Mechanics* **143** (2015), 121–137.